

# SECTION 2.2.7

## SEALLESS PUMPS

FREDERIC W. BUSE  
STEPHEN A. JASKIEWICZ

Sealless pumps are developed to eliminate the liquid leakage to the atmosphere that occurs from pumps that employ packing or mechanical seals. This leakage is usually toxic or dangerous to the environment. Sometimes the leakage is valuable. Eighty percent of the applications are for pressures below 200 lb/in<sup>2</sup> (13.8 bar) and below 250°F (120°C).

Sealless pumps are divided into two categories: magnetic drive pumps and canned motor pumps. The two categories compete against themselves in certain applications, but for the most part they each have their own market niche into which they are applied. Both have encapsulated inner driven mechanisms. On a magnetic drive pump (see Figure 5 in Section 2.2.7.1), the impeller is mounted to an inner magnet carrier. The inner and outer magnetic carriers are sealed by what is called a shell, which contains pump internal pressure. On a canned motor pump (see Figure 1 in Section 2.2.7.2), the impeller is mounted directly to the motor rotor. The atmospheric sealing element between the motor stator and rotor is called a liner or "can." Both magnetic drive and canned motor pumps use product lubricated bearings of compatible design and materials. These bearings are usually cooled and lubricated by the pump liquid.

The following sections describe both magnetic drive and canned motor pumps.

# SECTION 2.2.7.1

## MAGNETIC DRIVE PUMPS

FREDERIC W. BUSE

The principle of a magnetic drive pump is the elimination of the seal or packing in an overhung pump (Figure 1) and cutting the shaft in two at the seal location (Figure 2a). On the inner or wet end half of the shaft (Figure 2b), an inner magnet assembly (a) is placed on a shaft (b) supported by product lubricated bearings (c). On the other cut portion of the shaft, an outer magnet assembly (d) is placed on the power shaft (e). Between the inner and outer magnet assemblies, a static seal (f) isolates the shell (g) or diaphragm and the pumped liquid from the atmosphere. The magnetic flux from the outer magnet assembly drives the inner magnet assembly and impeller(s). The outer assembly is mounted directly to either its own bearing assembly in a frame housing (Figure 3) or motor shaft (Figure 4). Figure 5 shows a cross-section of a magnetic drive frame mounted pump.

**Magnetics** A magnetic circuit usually consists of two sets of permanent magnets and inner and outer conducting rings (Figure 6). The conducting rings can be cast iron, ductile iron, or a 400 series stainless steel.

**Magnet Materials** The first permanent magnets, developed in the 1940s, were made of aluminum-nickel-cobalt (AlNiCo) and used in small chemical pumps. Development of rare earth magnets in the 1980s made it possible to have a small power package that could drive larger pumps. The two types of rare earth materials commonly used are neodymium iron boron (NdFeB) and samarium cobalt (SmCo). The SmCo is four times stronger than AlNiCo. NdFeB, at 70°F (21°C), is 20% stronger than SmCo. The advantage of SmCo is the maximum service temperature of 550°F (288°C), almost twice that of NdFeB, which is 300°F (149°C). Figure 7 shows the strength versus temperature characteristics of the two materials. The cost of SmCo, however, is about twice that of NdFeB.

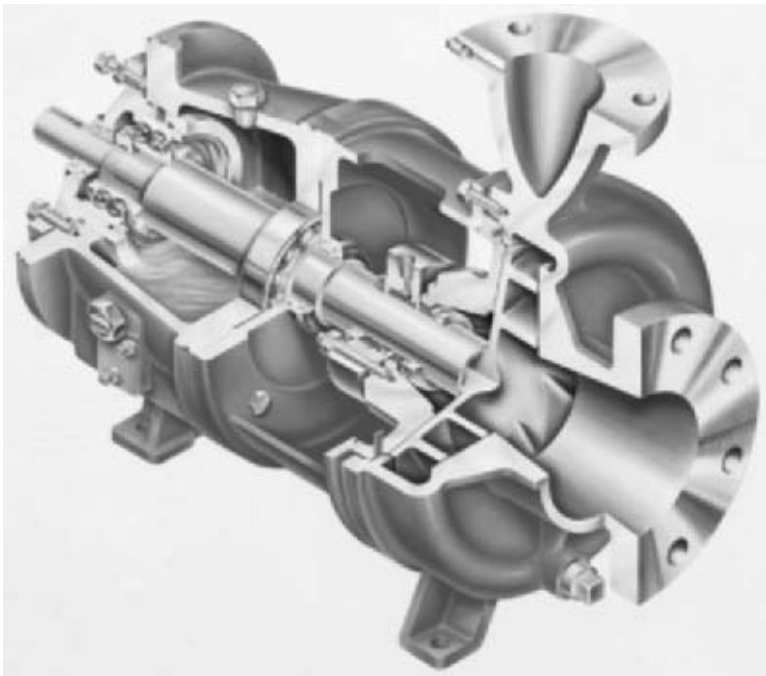


**FIGURE 1** Pump with conventional bearing housing and mechanical seal (Flowserve Corporation)

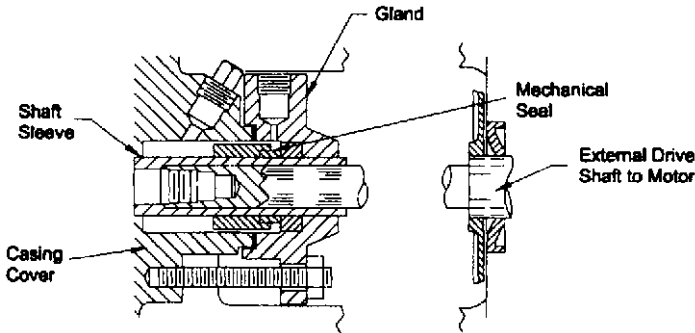
The magnets have a maximum temperature at which they lose all magnetism in an irreversible process; the magnets do not regain magnetism as they cool. This temperature is the Curie temperature and is shown for each magnet material in Table 1.

**TABLE 1** Operating and Curie temperatures for magnet materials

Type of Magnet Material	Operating Temperature (°F/°C)	Curie Temperature (°F/°C)
AlNiCo	660/305	800/425
NdFeB	250–300/120–137 (Depending on grade)	600/310
SmCo	500–660/260–350 (Depending on grade)	1300/700

**Conduction Ring** The amount of transmittal torque depends on the overall gap (Figure 8) between the poles of the magnets and the thickness of the conducting ring (Figure 9). If the thickness of the conducting ring is too small, it will become saturated with flux and the torque capability will be reduced.

A.



B.

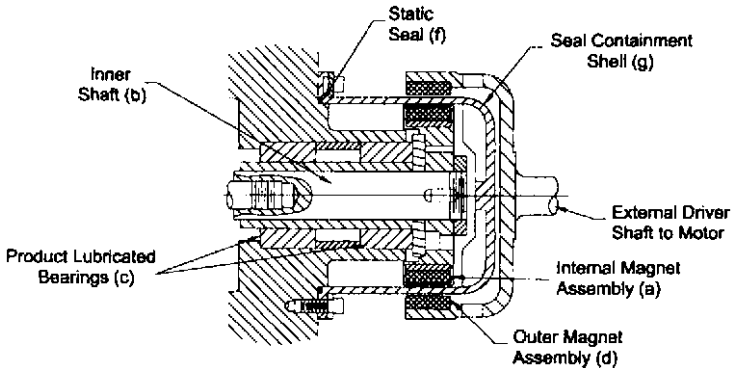


**FIGURE 2** Comparison of typical mechanical seal arrangement and sealless pump drive configuration: a) arrangement for typical mechanical through casing cover; b) sealless drive configuration

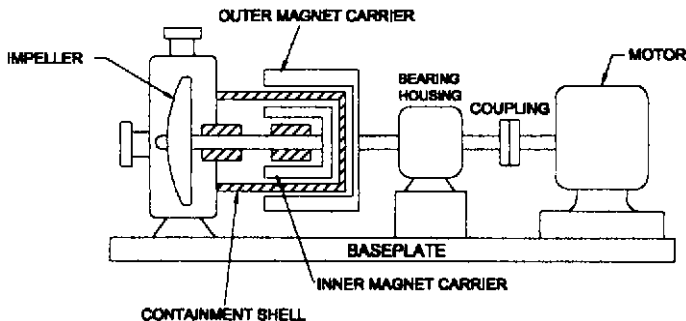


**FIGURE 3** Frame-mounted magnet drive arrangement

**Gap** The “overall gap” (Figure 10) is made up of the air gap, containment shell thickness, liquid gap, and encapsulation. Gap dimensions are based on the pressure requirement for the shell, the number of magnets (single or dual), and the material of the shell (metallic or nonmetallic) in the gap.

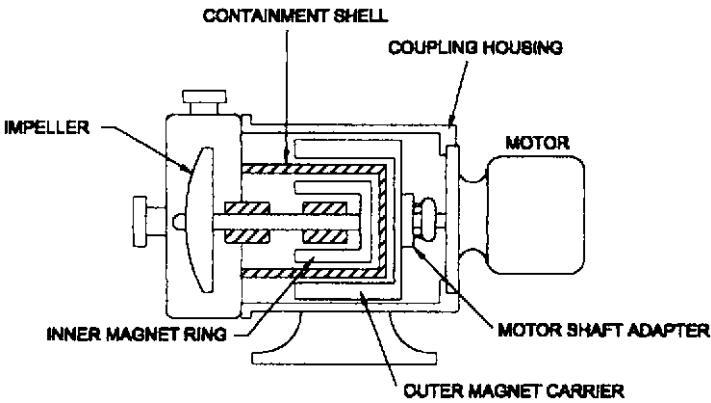


FIGURE 4 Close-coupled magnet drive arrangement

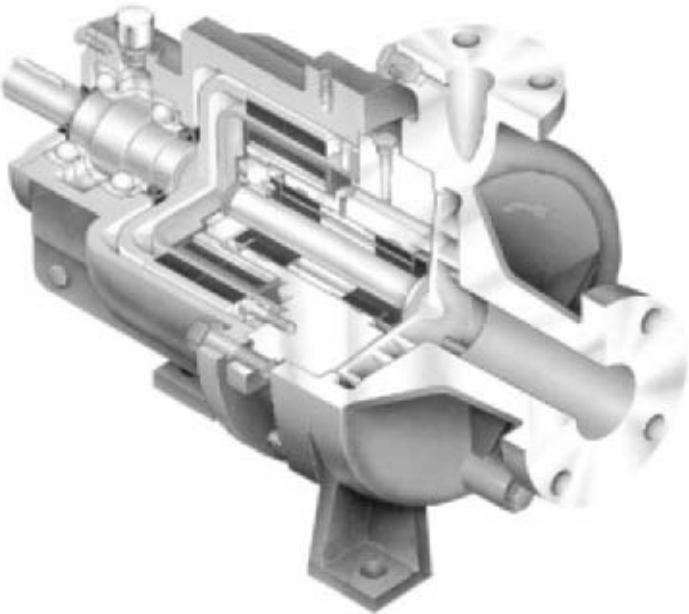


FIGURE 5 Cross-section of a frame-mounted magnet-driven pump (Flowserve Corporation)

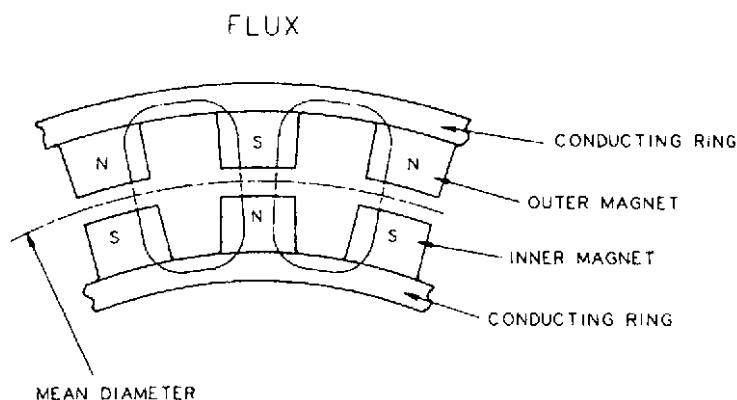


FIGURE 6 Magnetic circuit

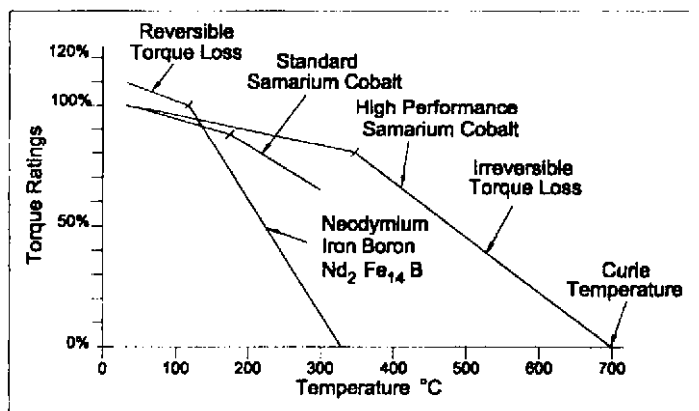


FIGURE 7 Magnet strength versus temperature

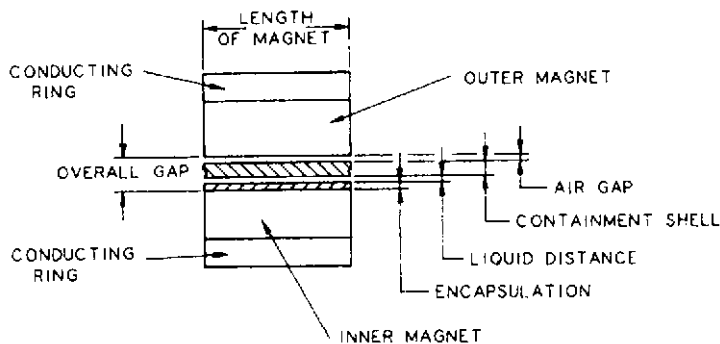


FIGURE 8 Magnet configuration

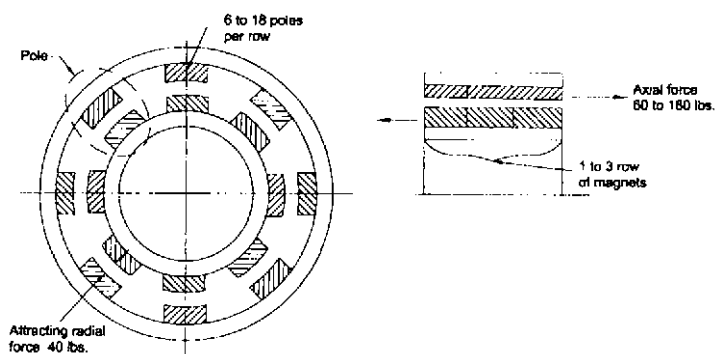
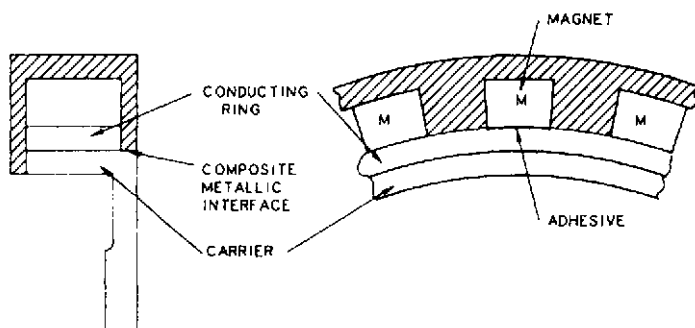
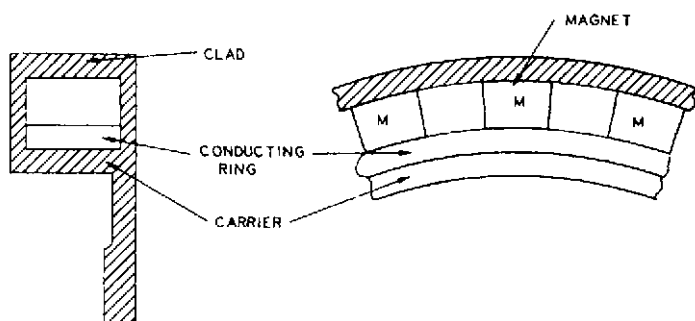


FIGURE 9 Rows of magnets



(A) NONMETALLIC COMPOSITE



(B) METALLIC

FIGURE 10A and B Encapsulation of magnets using nonmetallic composition and metallic clad

EXAMPLE Dimensions shown as in (mm)

Mean diameter (on radius dimensions)	4.6 (117)	6.0 (152.4)
Air gap minimum	.030 (0.762)	.045 (1.143)
Containment shell thickness: Hastelloy C	.040 (1.016)	.060 (1.524)
Polymer	.120 (3.048)	.150 (3.810)
Liquid gap	.035 (0.889)	.035 (0.889)
Encapsulation	.030 (0.762)	.030 (0.762)
Overall gap (basis Hastelloy C)	.135 (3.429)	.170 (4.318)
Overall gap (basis polymer)	.215 (5.461)	.260 (6.604)

In the previous example, the same overall gap was maintained for polymer and Hastelloy C shells. This allows for interchangeability of the magnetic assemblies independent of shell material.

**Transmittal Torque** The torque transmitted by the magnets depends on the following:

- Flux density of the magnets,  $B_g$
- Operating temperature of the magnets (which will change  $B_g$ )
- Length of the magnet poles,  $L$
- Number of magnets per ring,  $M$
- Mean ratios between the ID of the outer assembly magnets and OD of the inner assembly magnets,  $r$
- Overall gap between the ID and OD of the magnets in the assembly,  $g$
- A constant,  $K$ , which changes as a function of the specific design

Torque is determined from the following relationship, with appropriate units:

$$T = \frac{K \times B_g^2 \times L \times M \times r}{g}$$

For a given design type and configuration, the torque varies inversely as the square of the overall gap. Depending on costs and specific design construction, an assembly ring of magnets can have either one continuous length of magnets of a series of 1, 2, 3 or more rows of individual magnets.

## TORQUE CAPABILITY

The ultimate torque is the static “breakaway torque.” To determine this, the magnet carriers are assembled so the inner carrier is locked in position. Then a torque is applied by bar and weights or by a torque wrench to the outer carrier. The torque value at which the two carrier assemblies break loose from each other radially—or “decouple”—is called the “breakaway torque.” The designer has to account for the driver start-up acceleration time, start-up torque, and an appropriate safety factor to apply to the breakaway torque to determine the allowable applied torque.

Table 2 gives examples of the torque capability of assemblies composed of NdFeB blocks of magnet 0.75 in wide  $\times$  0.38 in high  $\times$  1.125 in long (19 mm  $\times$  9.65 mm  $\times$  28.6 mm) with a 0.180 in (4.6 mm) thick conducting ring.

**Basic Dimensioning of Magnet Blocks** The magnet blocks can be made too long or too short, resulting in handling, magnet molding, or flux density problems. The ratio of the dimensions for magnet blocks for successful designs is as follows:



**TABLE 2** Torque capability of magnet assemblies

Mean Diameter in (mm)	Magnets/Row	Overall Gap in (mm)	Breakaway Torque ft-lb (N • m)
4.3 (109)	12	0.240 (6.10)	30 (40)
6.0 (152)	18	0.260 (6.60)	60 (80)

**TABLE 3** Coefficients of thermal expansion (in/in/°F × 10<sup>-6</sup>)/(cm/cm/°C × 10<sup>-6</sup>)

Magnet material	Parallel to Axis	Perpendicular to Axis
NdFeB	5 (9)	9 (16.2)
SmCo	20 (36)	16 (28.8)

- Block width is two to three times the thickness.
- Block length is three to five times the thickness.
- Doubling the block thickness will increase the strength by approximately 20%.

For reference: 1.0 in<sup>3</sup> (16.387 cm<sup>3</sup>) of NdFeB per assembly at a mean diameter of 4.0 in (101.6 mm) with a 0.25 in (6.35 mm) overall gap produces approximately 7 ft-lb (9.5 N • m) of torque. A 3% reduction in flux density is equal to a 6% reduction in torque.

**Characteristics of magnet material:**

- Density: 0.273 lb/in<sup>3</sup> (7.56 g/cm<sup>3</sup>)
- Tensile: 12 × 10<sup>3</sup> lb/in<sup>2</sup> (844 kg/cm<sup>2</sup>)
- Compression: 110 × 10<sup>3</sup> lb/in<sup>2</sup> (7.7 × 10<sup>3</sup> kg/cm<sup>2</sup>)
- Flex stress: 36 × 10<sup>3</sup> lb/in<sup>2</sup> (2.53 × 10<sup>3</sup> kg/cm<sup>2</sup>)

Coefficients of thermal expansion are shown in Table 3.

**Radial and Axial Magnet Forces** The inner and outer carriers have to be restrained radially by bearings from contacting each other. In the example of “Torque Capability,” a single row of 18 magnets with a 6 in (152 mm) mean diameter, the radial force with magnets concentric is 40 lb (18 kgf). When the magnets are offset by .005 in (0.127 mm), the radial force is 55 lb (25 kgf) (Figure 9). When the magnets are against each other (no gap), the radial force is 80 lb (36 kgf).

In the previous example, it takes 60 lb (27 kgf) in an axial direction to separate a single row of concentric magnets and 180 lb (82 kgf) for three rows. It is strongly advisable that provisions be made for personnel to address these loads during assembly and disassembly of the carriers.

**Encapsulation of Inner Carrier Magnetics** Encapsulation can be accomplished with either metallic or polymer materials. The encapsulation of the inner magnet and conducting ring is probably the most expensive and extensive process in a magnetic drive sealless pump. After encapsulation, the carrier should be nondestructively tested to confirm 100% effectiveness.

The pros and cons of polymer encapsulation (Figure 10a) are as follows:

1. Limited to 250–300°F (120–150°C)
2. SmCo magnets are used because of the high exposure temperature when applying polymer over the magnets.

3. The overall gap is increased because of the required thickness of the polymer.
4. Magnets must be restrained mechanically on the conducting ring by adhesives or high-strength polymers around the magnets.
5. Polymers like PFA/PTFE or PEEK are more corrosive-resistant than most metals.
6. Production polymer construction is much less expensive than metallic construction.
7. Polymer tooling is expensive.

The pros and cons of metallic encapsulation (Figure 10b) are as follows:

1. Temperature rating can be 500°F (260°C).
2. Thickness of the encapsulation material over the magnets can be 0.030 in (0.76 mm).
3. Welding of the components can be conventional, electron beam, or laser. However, care must be taken with conventional welding to prevent the arc from jumping toward the magnet flux.
4. If castings are used for the inner carrier, porosity can be a problem.
5. Gassing of polymers from welding heat coming out of the seams can be a problem.
6. Adhesives are not required to keep the magnets in place at 3600 rpm with metallic encapsulation; the outer shield performs this function.

**Encapsulation of Outer Carrier Magnets** The magnets for the outer carriers do not have to be encapsulated (Figure 11). However, material like NdFeB has an infinity for water absorption that results in rusting and swelling. The magnets can then break loose and move in position relative to one another. It is highly recommended that they be encapsulated with an epoxy or metal sheathing for atmospheric protection and handling.

**Construction** The outer carrier can be a casting or fabrication. The carrier is attached to the power end shaft in the bearing housing (Figure 3) or directly to a motor shaft, which is then called *close coupled construction*. When attached to the bearing housing shaft, there is very little axial or radial load applied to the bearings. This lightly loaded condition can result in internal skidding of the rolling element bearings within their races, resulting in premature bearing failure. Therefore, it is best to preload the bearings with a spring to prevent skidding. This can be accomplished outside of the bearing by a spring-loading feature (Figure 11).

**Containment Shell** The containment shell shape and thickness depends on working pressure, material, and temperature. The shell thickness is usually uniform. To keep the

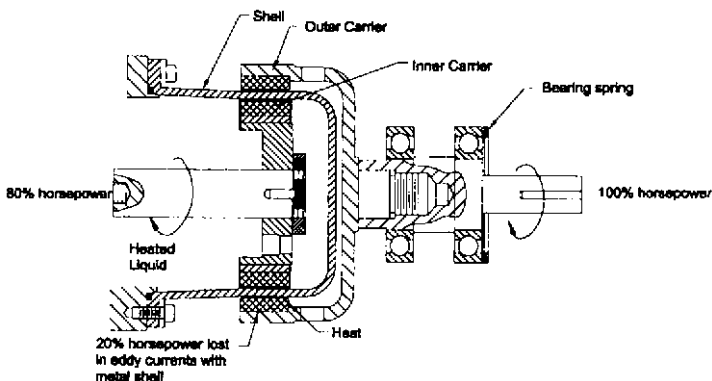


FIGURE 11 Inner and outer carrier

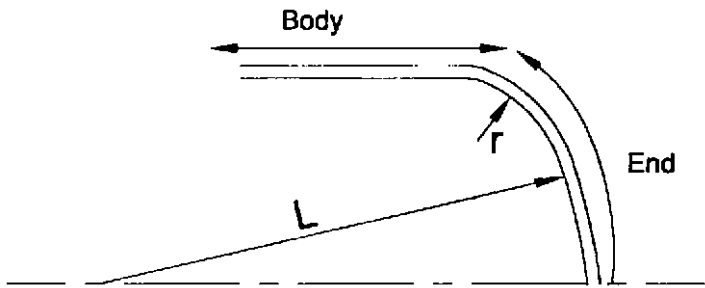


FIGURE 12 Shell ratio  $L/r$  for pressure

**TABLE 4** Pressure capabilities of shells with various end shapes for the same thickness and material

Shape	$L/r$	Allowable pressure—lb/in <sup>2</sup> (kPa)	Ratio of allowable pressure to that for a flat plate
Flat	533	9 (62)	1.0
Flat	267	23 (158)	2.55
Elliptical	28	113 (779)	12.6
Elliptical	8	209 (1440)	23.2
Spherical	1	815 (5620)	90.5

length of the shell to a minimum, a square-ended shell can be used. However, unless the end of the shell is made extra thick, it would have a relatively low pressure capability. Therefore, an end shape which is elliptical or spherical is used to obtain higher pressure capability (Figure 12).

Examples of how allowable shell pressure varies with the shape of the end plate are shown in Table 4.

The classes of materials used for containment shells (Figure 11) include metals, polymers, and ceramics. The characteristics of containment shells of various materials are shown in Table 5. The main advantage of polymer or ceramic shells is that there are no eddy current losses. Therefore, cooling of the magnets is not required.

**Eddy Currents** Metallic or metallic-lined shells will produce eddy currents. Depending on the thickness of the shell, the eddy current losses ( $P_L$ ) can amount to as much as 20% of the total power.

$$P_L = \frac{K \times T \times L \times N^2 B_g^2 D^3 M}{R}$$

where  $K$  = a constant, depending on the design

$T$  = thickness of the shell

$L$  = length of magnets (times the core of magnets)

$N$  = speed, rpm

$B_g$  = flux density of the magnets

$D$  = mean diameter

$M$  = number of sets of magnets

$R$  = electrical resistivity, microhms per cm<sup>3</sup> (electrical resistivity for various shell materials is given in Table 6)

**TABLE 5** Characteristics of containment shells of various materials

Material	Metal	Reinforced polymer	Ceramic	Metal with PTFE
Construction	Welded or hydroformed	Injection molded	Set and fired	Spray coated
Temperature limit—°F (°C)	−300 to + 750 (−150 to +400)	−40 to +250 (−4 to +120)	32 to 2000+ (0 to 1100+)	32 to 350 (0 to 175)
Thickness—in (mm)	0.030–0.040 (0.76–1.0)	0.170 (4.3)	0.250–0.380 (6.35–9.6)	0.050 (1.27)
Heat conductivity*	Hastelloy C = 71 AISI 316 = 7.5	3	6	Higher than metal alone
Creep	None	None	None	Some
Thermal shock	1000+ (537+)	375 (190)	500 (260)	—
Eddy currents	316 is twice Hastelloy C	None	None	Same as metal

\*Approximate thermal conductivity in Btu/hr/ft<sup>2</sup>/°F. Multiply by 0.488 to get calories/hr/cm<sup>2</sup>/°C

**TABLE 6** Electrical resistivity of various shell materials

Shell Material	Electrical Resistivity ( <i>R</i> ), microhms per cm <sup>3</sup>
Hastelloy C	130
AISI 316L	74
Inconel 625	129
Nimonic 90	115
Titanium	53
K-Monel	58
Alloy 20	75

**TABLE 7** Effect of material selection on heat build-up

Material of shell	Thickness-in (mm)	Time-minutes	kW	°F (°C)	°F/min (°C/min)
AISI 316	0.43 (10.9)	Start	0.40	80 (27)	—
AISI 316	0.43 (10.9)	5.0	0.30	500 (260)	100 (38)
Hastelloy C	0.43 (10.9)	0.5	0.24	170 (77)	340 (171)
Hastelloy C	0.43 (10.9)	5.0	0.21	370 (188)	74 (23)

The effect of material selection on heat build-up is shown in Table 7. The tabulation shows the temperature rise of the air space inside a shell with only the outer carrier spinning around a metallic shell (no inner carrier in place) at 3550 rpm. The carrier has 12 magnets, 1.25 in (3.175 cm) long, with a mean diameter of 4.25 in (11.43 cm).

This illustrates the difference between AISI 316 and Hastelloy C shells at 3550 rpm. At 1750 rpm, the power loss for AISI 316 would be one-fourth that at 3550 rpm, which may not result in excess power consumption.

There are also axially laminated metal shells available that substantially reduce eddy current ( $I^2R$ ) losses. These laminations work on the principle that when a shell length is

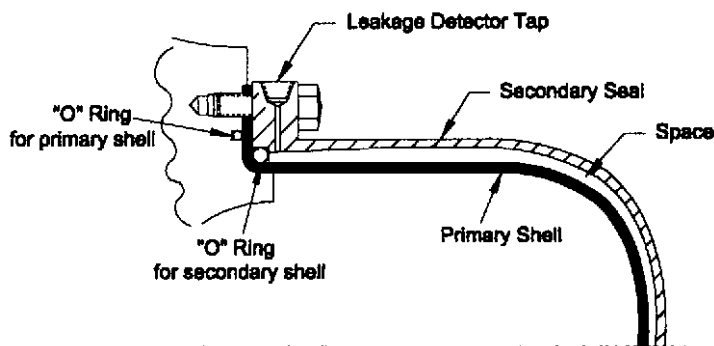


FIGURE 13 Dual containment

cut in half, the eddy current losses are reduced to one-fourth their original value. If the one-half shell length is cut in half again, the resulting pieces have eddy current losses one-sixteenth that of the original shell. A shell design made of segments sealed together to make a full-length shell will thus reduce total eddy current losses.

**Dual Containment** As a precaution against leakage due to a breach in the primary containment shell, a dual or double-containment arrangement can be used. This double layering of shells (Figure 13) usually consists of a combination of a nonmetallic and metallic shell. The pressure rating of the secondary shell is equal to that of the primary shell. It is designed to operate at least 48 to 120 hours after a breach in the primary shell occurs. A pressure monitor is inserted in the flange of the secondary shell to detect pressure buildup from primary shell leakage.

**Bearings** The internal shaft system of the pump is supported by one or more bearings. Some designs use a rotating shaft; others use a mandrel on which the bearings rotate. The bearing, which consists of a journal and bushing, is made of various materials, depending on the loads and pumpage (used for product lubrication). The bearing loads are from the weight of the components and hydraulic forces from the impeller and inner carrier. The impeller forces are both radial and axial.

Most magnetic drive sealless pumps are single-stage volute pumps that have the same radial bearing loads as comparable conventionally sealed pumps. The main difference with the sealless pump is that there is almost no overhang from the impeller to the first bearing. The load on the bearing, therefore, is almost equal to that of the impeller. In a conventionally sealed pump, the load on the radial bearing is almost twice that of the impeller. This can be seen by comparing Figures 1 and 5.

The axial load will depend on whether the impeller is enclosed or semi-open (Figure 14). Enclosed impellers usually have horizontal front rings and may also have a back ring or pump out vanes (POV). Semi-open impellers have no rings, but they usually employ scallops in the shroud to reduce the effective pressure area (Figure 15). Axial thrust force is further reduced by employing pump-out vanes (POV) or pump-out slots (POS) on the back shroud of the impeller to reduce the amount of pressure on the impeller back shroud.

The enclosed impeller can have less radial and axial load than a semi-open impeller. This is usually accomplished by employing back rings (14b). To ensure positive pumping in the lubrication flow path in magnetic drive pumps, POV-POS on an enclosed or semi-open impeller are recommended.

Liquids pumped in chemical or petroleum plants may have low viscosity, low specific gravity, or low specific heat. These characteristics can result in boundary lubrication rather than hydrodynamic lubrication of the product lubricated bearings. Therefore, bearings are selected using PV (pressure-velocity) values. Some limiting PV values for various bearing material combinations are shown in the following section on bearing materials.

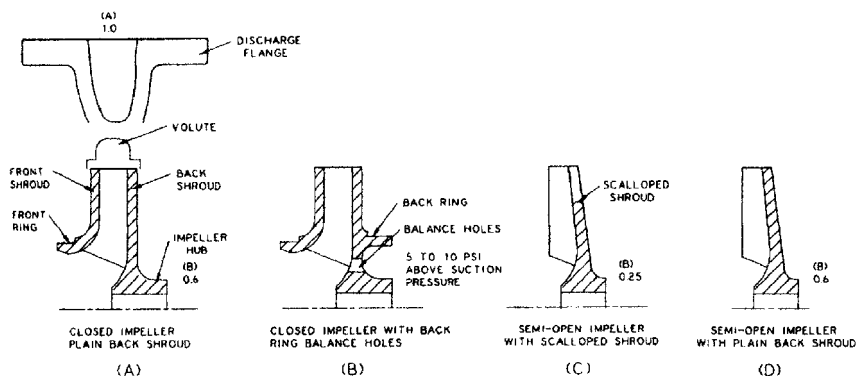


FIGURE 14A through D Various enclosed and semi-open impeller configurations

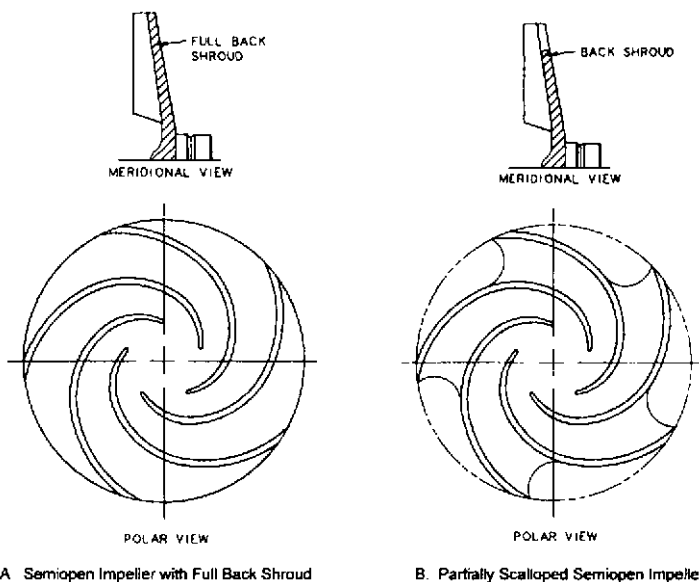


FIGURE 15A and B Semi-open impellers with a full back shroud and with a partially scalloped back shroud

**Bearing Materials** Table 8 shows PV values for various bearing journal and thrust face materials. When loads exceed a PV value of 150,000, the bearing should have an alignment compensator built in to correct for inaccuracies in perpendicularity, concentricity, and parallelism of parts.

When designing the bearing, thermal expansion and heat conductivity properties must be considered. Some designs have a temperature range of  $-300^{\circ}\text{F}$  to  $+750^{\circ}\text{F}$  ( $-150$  to  $+400^{\circ}\text{C}$ ). Table 9 lists bearing material characteristics to facilitate selection of the proper material for the intended application.

**Particles** For the softer bearing materials, the maximum particle size should be no more than 10% of the diametral clearance for a bearing with no grooves and no more than 20%

**TABLE 8** PV values for various bearing journal and thrust face materials

Bushing Materials	Journal/Thrust Face PV ( $\times 10^3$ )*
Carbon Graphite vs. AISI 316	150
Carbon Graphite vs. Chrome Oxide Hardened Coating	250
Silicon Carbide vs. Hardened Coating	250
Silicon Carbide vs. Carbon Graphite	300
Silicon Carbide vs. Silicon Carbide	500
PEEK—Carbon-filled vs. Hardened Coating	150
Polyimide-carbon filled vs. Hard Coating	150

$P$  = Net load/projected area (minus area for slots), psi

$V$  = Velocity at the shaft diameter or mean diameter of the thrust face in ft/min

\*Note: Multiplying the PV values in the table by 2.1 will give values equal to  $P$  in kPa and  $V$  in m/min.

**TABLE 9** Bearing material characteristics

Material	Thermal Expansion (note 1)	Heat Conductivity (note 2)	Hardness (note 3)
AISI 316	9.6	7.5	160 BHN
Hastelloy C	6.7	71	170 BHN
Carbon graphite	2.6	5	95 Vickers
Silicon carbide— self-sintered	2.2	85	2400 Vickers
Silicon carbide with carbon	2.0	75	2400 Vickers
PEEK—Carbon-filled	8.0	6	
Polyimide—Carbon-filled	5.0		100–150 BHN
Aluminum oxide			1800 Vickers
Chrome oxide			1800 Vickers

Note 1: in/in/°F  $\times 10^{-6}$  (multiplied by 1.411 to get cm/cm/°C)

Note 2: BTU/hr/ft<sup>2</sup>/°F (multiply by 0.488 to get calories/hr/cm<sup>2</sup>/°C)

Note 3:  $R_C \times 25$  = Vickers; BHN  $\times 10$  =  $R_C$

for a bearing with grooves. Polymers and graphites are much softer than silicon carbides or hard coatings, and they are not recommended for liquids with hard particles. Silicon carbide versus silicon carbide will grind up most particles. For particle concentrations of 50 parts per million (ppm) or less, particle hardness is generally not a factor in bearing performance.

Strainers of 100 mesh are recommended to reduce the amount and size of particles going through the flow path. These strainers are installed for internal or external injection. Remember: Particles that will pass through a 100 mesh screen may be as large as 0.006 in (0.15 mm), whereas nominal diametral bearing clearances of 0.002 in (0.05 mm) are common.

Note also that the bearing material combination of silicon carbide against silicon carbide or against carbon is electrically conductive.

**Running Dry** Most sealless pump failures occur because the pump system is not monitored and the pump is allowed to run dry. When this happens, the bearings will run dry. When the bearings run dry, hard, brittle bearing materials such as self-sintered silicon

carbide will fail within minutes. Graphite silicon carbide may run dry for as many as 10 to 20 minutes with no damage. The polymers, which are poor heat conductors, expand inwardly and seize against the mating surface. The graphites will also move inwardly, but they tend to wear rather than seize, which results in excessive clearances when the pump is stopped and cooled. One optional design uses Teflon strips that expand inwardly when the unit runs dry so the shaft runs on the Teflon rather than on the silicon carbide, thus helping to avoid bearing failure.

Another option is to employ an external circulating tank, with no external running parts, that will provide the bearings with external lubricating liquid should dry operation occur. This type of external tank system has allowed pumps to operate for two hours or more without incurring damage to the bearings.

**Flow Path** The amount and direction of flow for cooling of the magnets and lubrication of the bearings is critical to the operation of a sealless pump (Figure 16). It is preferable for the liquid to lubricate the bearings before being heated by the magnets. This reduces the possibility of vaporization of the liquid occurring at the thrust-bearing faces. The amount of liquid circulated through the system is usually between 1 and 8 gpm (4 and 30 l/min). It is usually channeled to the front and back bearings, the thrust bearing face, across the magnets, and to the impeller hub. Some manufacturers have computer programs that calculate the flow, pressure, and temperature of the cooling/lubricating flow at various critical locations along the flow path. These programs can also account for the effects of the liquid specific gravity, specific heat, and viscosity. The local pressure and temperature is used to determine the vapor pressure at that point to ensure that the liquid is not flashing. The programs can also calculate axial thrust and determine if the lubrication at the thrust bearing face is hydrodynamic or boundary. This is done at various flow rates, impeller diameters, and pump speeds.

The temperature rise of the liquid as it travels through the cooling-lubricating flow path depends to a great extent on the liquid's characteristics, such as specific gravity, specific heat, vapor pressure, and viscosity. With a nonmetallic shell on ambient water service, a typical temperature rise might be 1 to 2°F (0.5 to 1°C). For a metallic shell, with its much higher eddy current losses, the temperature rise could be as much as 8 to 12°F (4 to 7°C).

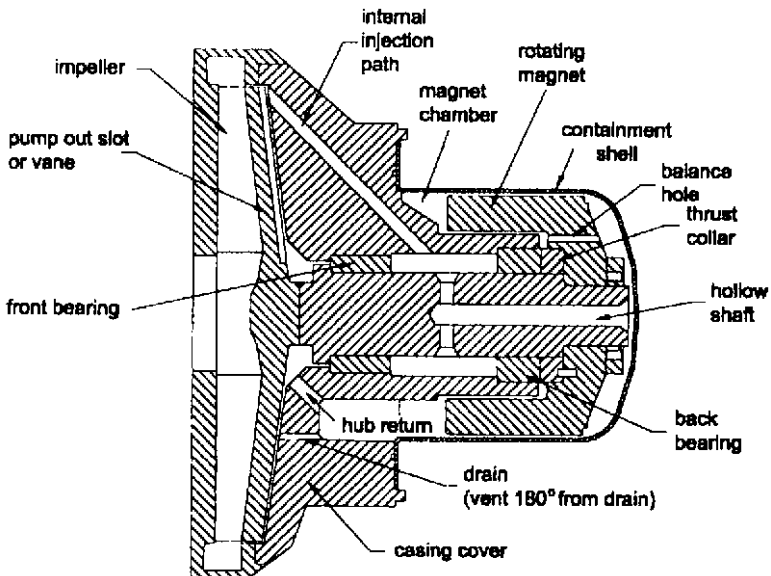
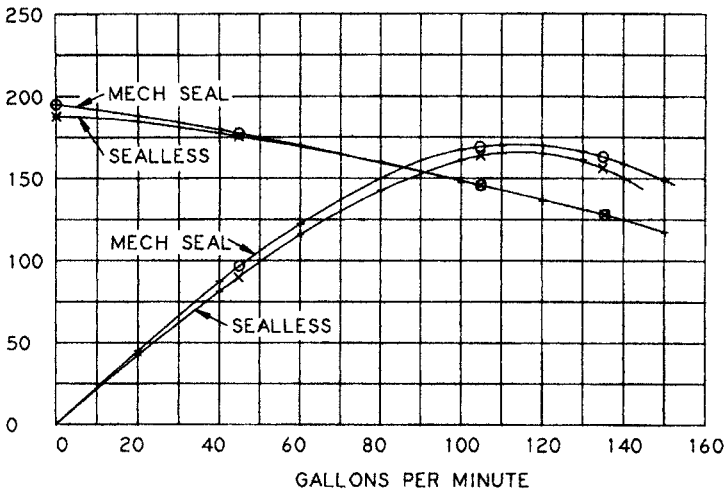


FIGURE 16 Magnetic sealless pump components for the internal flow system





**FIGURE 17** Typical performance for a  $1.5 \times 1.0 \times 6$  pump at 3550 rpm, comparing characteristics for sealless versus mechanical seal construction

**Performance** The head capacity curve of a typical two-pole speed sealless pump matches that of a conventionally sealed pump; however, the overall efficiency is lower. With a nonmetallic shell, the efficiency may be only about two points less at the best efficiency point flow rate, but as much as six points less at one-half the best efficiency point flow rate. When a metallic shell is used, the efficiency at best efficiency point flow rate may be as much as 8 to 12 points lower than a comparable pump with a mechanical seal (Figure 17).

#### APPLICATION ADVANTAGES OF SEALLESS PUMPS:

- No leakage to the environment
- No loss of valuable liquids
- Lower noise levels
- High suction pressure does not affect the axial thrust
- Can handle liquids from 0 to 4 toxicity rating
- Because of no leakage, there is much less chance of a fire
- Easier to obtain construction permits and permits for continued operation
- Less external piping required

#### APPLICATIONS THAT SHOULD BE REVIEWED BEFORE SEALLESS PUMPS ARE APPLIED:

- Dirty liquids
- High temperature
- Liquids that solidify
- Viscous liquids above 200 centipoise
- Oversize drivers that can cause decoupling during acceleration
- Cavitation of liquid in the impeller eye that can result in excess thrust
- Excessive entrained gas

**REFERENCES AND FURTHER READING**

---

1. American National Standard for Sealless Centrifugal Pumps, ANSI/HI 5.1–5.6-2000, Hydraulic Institute, Parsippany, NJ [www.pumps.org](http://www.pumps.org).
2. Hydraulic Institute ANSI/HI 2000 Edition Pumps Standards, Hydraulic Institute, Parsippany, NJ [www.pumps.org](http://www.pumps.org).
3. Sealless Pumps for Petroleum, Heavy Duty Chemical, and Gas Industry Services, API Standard 685, 2000, The American Petroleum Institute, 1220 L Street, Northwest, Washington, D.C. [www.api.org](http://www.api.org).
4. Specification for Sealless Horizontal End Suction Centrifugal Pumps for Chemical Process, ANSI/ASME B73.3M-1997, The American Society of Mechanical Engineers, 345 East 7th Street, New York, NY [www.ASME.org](http://www.ASME.org).
5. Eierman, R. "A User's View of Sealless Pumps—Their Economics, Reliability, and the Environment." *Proceedings of the Seventh International Pump Users Symposium*. Texas A&M University, College Station, TX, March 1990, pp. 127–133.
6. Hernandez, T. "A User's Engineering Review of Sealless Pump Design Limitations and Features." *Proceedings of the Eighth International Pump Users Symposium*. Texas A&M University, College Station, TX, March 1991, pp. 129–145.
7. Littlefield, D. "Sealless Centrifugal Pumps." *Proceedings of the Eleventh International Pump Users Symposium*. Texas A&M University, College Station, TX, March 1994, pp. 115–119.
8. Guinzburg, A., and Buse, F. "Computer Simulation of the Flowpath in Magnetic Sealless Pumps." *Proceedings of the Fifteenth International Pump Users Symposium*. Texas A&M University, College Station, TX, March 1998, pp. 1–9.